Geostrophic and Tidal Currents in the South China Sea, Area III: West Philippines

Anond Snidvongs

Department od Marine Science, Chulalongkorn University, Bangkok 10330, Thailand

Introduction

Physical oceanography is an important environmental factor controlling fishery productivity and fishing potential of a fishing ground. Thus, in this SEAFDEC Collaborative Research Program, physical oceanography has always been included.

Study Area

The study area II of the Collaborative Research was along the western coast of Luzon and Palawan Islands, in the Exclusive Economic Zone of the Philippines. The bathymetry of the area indicated the bottom depth up to more than 4000 m (Fig 1). The area is part of the South China Sea connected to the Pacific Ocean through the Bashi Strait to the north, and the lesser extent through the Visayas Sea. In addition, the area is also connected to the Sulu Sea to the south.

Water circulation in the surface mixed layer of the South China is strongly influenced by prevailing wind (Asian Monsoon and Pacific Trades). Generally the surface water flows northward during the Southwest Monsoon and opposite during the Northeast Monsoon. It is not clear, however, about the orographic effect from the near-by landmass on the Ekman circulation in the study area.

SEAFDEC Cruise No. 50 took place from mid April to mid May 1998, the intermediate period between Northeast and Southwest Monsoons. During the first half of the survey which was in the northern part, the wind was generally from the north and east through the Bashi Strait while during the last half of the survey in the southern part, the wind was generally from the east through the Visayas Area (Fig 2).

Data Collection and Calculations

CTD cast was carried out at all 31 stations using the onboard Falmouth CTD system. Calibrations were not performed due to limitation of funding and lack of suitable high precision calibration instrument. Raw data was averaged at every 1 dbar. Salinity and dynamic height were calculated based on standard equation of state of seawater using the EG&G Post Acquisition Data Analysis Software. Missing values and noises, if occurred, were substituted by binomial interpolation.

For the calculation of relative geostrophic current at each station, where the level of no-motion was assumed at 1000 dbar, data from Stations 3, 23, 24, 25, 30A and 31A were excluded. At each station, the east-west velocity component (u) and north-south velocity component (v)

were calculated from dynamic slope to the east and to the north of the station, respectively. Steady state was assumed for the dynamic topography and therefore pressure gradient equal Coriolis force according to

$$g \tan(\theta) = fv \qquad \text{———— (1)}$$

where: g = gravitational acceleration (9.8 m s^{-2})

θ = dynamic topographic slope = dynamic height difference between stations divided by distance

f = Coriolis parameter, $1.455 \times 10^{-4} \sin(\text{latitude})$ s^{-1}

v = velocity, m s^{-1}

Cartesian coordinate system was used, i.e. the vector was positive eastward and northward. A total of 14 stations (1, 5, 6, 7, 10, 11, 12, 13, 14, 18, 19, 20, 21, and 27) had sufficient data to satisfy the calculation.

In addition to geostrophic balance calculation, the actual half-hourly currents at 3 levels (10m, 50m and 100m) over diurnal cycle were observed at Stations 1, 5, 12, and 27. Because the water depth was too large for the bottom tracking mode, the Furuno Doppler Current Indicator was operated in the relative mode, i.e. the recorded currents were relative to surface current at that time.

The observed relative current data was decomposed into u and v vectors. These vectors were smoothened by 3-points running average. Harmonic analysis of these relative vectors for absolute tidal current parameter (diurnal and semidiurnal amplitudes and phases) was done on these relative vectors from all 3 layers according to:

$v'_{10} + v'_{50} + v'_{100}$
= *absolute v at 10 m - absolute v at 0 m + absolute v at 50 m - absolute v at 0 m + absolute v at 100 m - absolute v at 0 m*

$$= \langle v' \rangle_{10} + A_{1,10} \cos(2\pi\, t/T_{1,10} + \phi_{1,10}) + A_{2,10} \cos(2\pi\, t/T_{2,10} + \phi_{2,10})$$
$$+ \langle v' \rangle_{50} + A_{1,50} \cos(2\pi\, t/T_{1,50} + \phi_{1,50}) + A_{2,50} \cos(2\pi\, t/T_{2,50} + \phi_{2,50})$$
$$+ \langle v' \rangle_{100} + A_{1,100} \cos(2\pi\, t/T_{1,100} + \phi_{1,100}) + A_{2,100} \cos(2\pi\, t/T_{2,100} + \phi_{2,100})$$
$$- 3(A_{1,0} \cos(2\pi\, t/T_{1,0} + \phi_{1,0}) - A_{2,0} \cos(2\pi\, t/T_{2,0} + \phi_{2,0})) \qquad \text{———— (2)}$$

where v' = relative u or v component recorded by current meter (dependent variable)

t = time (independent variable)

$\langle v' \rangle$ = average v' (known constant)

A_1, A_2 = amplitudes of semidiurnal and diurnal components (unknown)

T_1, T_2 = periods of semidiurnal and diurnal components (unknown)

ϕ_1, ϕ_2 = phases of semidiurnal and diurnal components (unknown)

subscripts 0, 50 and 100 are for depths of 0, 50 and 100 meters

Least square method was used to fit Eq. 2 to the observed data.

Results

Dynamic topography at sea surface clearly shows a strong high dynamic surface between about 15° and 16° N and a strong low dynamic surface between 18° - 19° N latitudes (Fig 3). These low and high surfaces could reflect anticyclonic (clockwise) and cyclonic (counterclockwise) circulation, possibly due to eddies. The average speed of surface geostrophic

Table 1. The geostrophic current speed and direction at or near standard depths

z	St 1		St 5		St 6		St 7		St 10		St 11		St 12	
(m	m/s	dir	m/s	dir	m/s	dir	m/s	dir	m/s	dir	m/s	dir	m/s	dir
0	0.33	215.	0.22	347.	0.27	137.	0.48	049.	0.20	073.	0.31	092.	0.23	101.
10	0.33	215.	0.22	345.	0.26	137.	0.47	049.	0.20	074.	0.31	092.	0.23	101.
20	0.33	216.	0.21	344.	0.25	137.	0.46	049.	0.19	074.	0.31	092.	0.23	100.
30	0.32	217.	0.19	344.	0.24	133.	0.43	049.	0.19	074.	0.30	092.	0.23	100.
50	0.28	218.	0.15	343.	0.19	129.	0.34	047.	0.19	071.	0.29	093.	0.22	099.
70	0.22	215.	0.13	344.	0.15	124.	0.27	043.	0.16	065.	0.25	096.	0.19	095.
10	0.13	205.	0.11	350.	0.12	116.	0.19	036.	0.13	054.	0.18	105.	0.12	092.
13	0.07	182.	0.11	355.	0.10	114.	0.15	026.	0.11	043.	0.14	117.	0.08	096.
15	0.06	164.	0.11	358.	0.09	113.	0.13	021.	0.11	039.	0.13	123.	0.06	098.
20	0.06	117.	0.10	000.	0.07	108.	0.09	012.	0.09	033.	0.11	135.	0.04	099.
25	0.08	104.	0.09	000.	0.06	102.	0.06	005.	0.07	028.	0.09	139.	0.03	102.
30	0.09	099.	0.08	358.	0.04	103.	0.04	005.	0.05	028.	0.07	140.	0.01	110.
40	0.10	102.	0.07	355.	0.02	127.	0.02	023.	0.02	021.	0.04	130.	0.00	182.
50	0.09	100.	0.06	354.	0.02	150.	0.02	056.	0.00	213.	0.03	109.	0.01	204.
60	0.08	095.	0.04	353.	0.01	180.	0.02	073.	0.01	211.	0.02	085.	0.01	203.
70	0.06	090.	0.03	347.	0.02	192.	0.02	079.	0.01	209.	0.01	069.	0.00	214.
80	0.04	079.	0.02	345.	0.01	186.	0.01	077.	0.01	206.	0.01	058.	0.00	276.
90	0.02	074.	0.01	334.	0.00	174.	0.01	064.	0.00	203.	0.00	070.	0.00	278.

z	St 13		St 14		St 18		St 19		St 20		St 21		St 27	
(m	m/s	dir	m/s	dir	m/s	dir	m/s	dir	m/s	dir	m/s	dir	m/s	dir
0	0.04	012.	0.14	174.	0.35	240.	0.38	277.	0.21	051.	0.22	049.	0.16	334.
10	0.04	015.	0.16	205.	0.24	248.	0.38	264.	0.21	051.	0.22	049.	0.16	337.
20	0.04	015.	0.15	205.	0.24	247.	0.38	264.	0.20	050.	0.22	048.	0.15	339.
30	0.04	011.	0.15	204.	0.25	246.	0.38	265.	0.20	050.	0.22	048.	0.15	342.
50	0.03	011.	0.14	201.	0.25	245.	0.36	266.	0.16	047.	0.21	044.	0.15	351.
70	0.04	008.	0.14	197.	0.22	242.	0.28	268.	0.08	028.	0.18	045.	0.17	359.
10	0.05	356.	0.12	192.	0.18	236.	0.15	280.	0.03	324.	0.16	046.	0.18	005.
13	0.04	339.	0.12	187.	0.14	230.	0.09	296.	0.04	296.	0.13	048.	0.18	013.
15	0.04	332.	0.12	185.	0.13	228.	0.08	308.	0.04	293.	0.12	052.	0.18	014.
20	0.03	319.	0.11	182.	0.11	221.	0.06	321.	0.04	294.	0.10	063.	0.16	014.
25	0.03	315.	0.09	179.	0.10	215.	0.05	326.	0.03	299.	0.08	071.	0.14	013.
30	0.02	326.	0.08	177.	0.09	212.	0.05	332.	0.03	310.	0.06	078.	0.12	011.
40	0.03	349.	0.06	176.	0.07	210.	0.04	336.	0.02	335.	0.04	093.	0.08	008.
50	0.02	358.	0.04	174.	0.06	212.	0.03	331.	0.02	345.	0.02	098.	0.05	356.
60	0.02	358.	0.03	171.	0.05	218.	0.03	331.	0.01	351.	0.01	091.	0.04	347.
70	0.01	359.	0.02	158.	0.04	225.	0.03	338.	0.00	348.	0.01	081.	0.02	352.
80	0.01	004.	0.01	169.	0.02	230.	0.01	332.	0.00	070.	0.01	068.	0.01	333.
90	0.00	007.	0.00	178.	0.01	232.	0.00	319.	0.00	056.	0.00	044.	0.00	274.

current around these eddies were in the range of 0.3 - 0.4 m s^{-1}. The remnant of these eddies could be observed as deep as 500 meter, where the geostrophic velocities were between 0 - 0.05 m^{-1} (Table 1).

The cyclonic eddy found near the head of Luzon Island was due to wind turbulence as the low altitude airmass was forced by Northeast Trade Wind in the Pacific into the South China Sea through the Bashi Channel between Taiwan and Luzon Islands. This turbulence driven cyclonic eddy in this part of the South China Sea was likely to be a regular annual feature that will effect ecology and fisheries production in the area.

The dynamic high off the west coast of central Luzon could be the result of the westerly wind from Pacific Ocean through the Visayas Area. On entering the South China Sea, the northern portion of this wind stream bent toward the Northwest and causing the net surface Ekman transport toward the west coast of Luzon. The generally southward transport due to wind turbulence near the head of the Island could further strengthen the convergence and thus high dynamic surface was observed.

While dynamic topography and geostrophic balance calculation represented more to a longer term of water circulation, as resulted from dynamic equilibrium between the atmosphere

Table 2. Harmonic constants for u and v components of tidal current

St	z (m)	vector	T_1 (h)	A_1 (m/s)	ϕ_1 (deg)	T_2 (h)	A_2 (m/s)	ϕ_2 (deg)
1	0	u	24.26	0.384	2.6	11.81	0.507	1.4
		v	23.23	0.048	103.0	11.63	0.028	34.4
	10	u	24.17	0.393	0.8	11.82	0.519	4.3
		v	23.92	0.077	121.1	12.00	-0.037	227.9
	50	u	24.28	0.378	2.6	11.80	0.523	-1.8
		v	25.52	0.132	-70.7	8.55	-0.072	-58.4
	100	u	24.52	0.421	-9.0	11.79	0.489	-3.3
		v	2061	-0.202	86.6	8.48	0.111	-272.2
5	0	u	24.26	0.384	2.6	11.81	0.507	1.4
		v	23.68	-0.125	-43.1	13.13	-0.129	93.5
	10	u	24.17	0.393	0.8	11.82	0.519	4.3
		v	23.89	-0.112	-30.4	13.20	-0.124	86.0
	50	u	24.28	0.378	2.6	11.80	0.523	-1.8
		v	21.85	0.080	57.1	13.92	0.107	-31.2
	100	u	24.52	0.421	-9.0	11.79	0.489	-3.3
		v	16.49	0.308	-99.1	15.67	0.360	48.9
12	0	u	25.00	-0.798	2.2	12.40	-0.298	-2.8
		v	26.10	0.724	-172.5	12.37	0.019	-26.8
	10	u	25.08	-0.798	-0.5	12.47	-0.250	1.7
		v	26.10	0.178	-114.9	26.14	-0.609	-2.4
	50	u	25.01	-0.805	1.1	12.42	-0.293	-3.8
		v	26.02	-0.771	1.1	14.68	-0.008	18.2
	100	u	25.00	-0.777	-2.6	12.39	-0.309	4.6
		v	25.99	-0.783	0.8	12.24	0.014	19.2
27	0	u	25.95	0.031	135.1	12.61	0.051	-104.9
		v	27.94	0.032	152.4	11.98	0.035	-6.8
	10	u	12.67	0.032	-116.4	8.34	-0.014	-106.5
		v	58.32	0.009	13.6	8.27	-0.031	-64.0
	50	u	24.72	-0.089	21.4	11.76	0.026	100.1
		v	24.88	-0.113	62.8	11.86	-0.051	-105.2
	100	u	24.37	-0.130	49.7	12.06	-0.043	24.4
		v	24.48	0.089	-57.5	13.47	0.010	-99.3

and the water, instantaneous current as observed at a moment in time would reflect more to the tidal and local winds which exerted a shorter time and space scale, and thus was less likely to reach the equilibrium. The characteristics of the tidal current are summarized in Table 2.

Tidal current at the sea surface was dominated by east-west diurnal component at St 1 with the maximum magnitude of about 0.5 ms^{-1} (Fig 4). The diurnal component became more dominant as the latitude decreased. At St 12, the northeast-southwest vectors were very prominent, over 1 m s^{-1}. Surface tidal current was negligible at St 27.

At 50-meter depth, tidal current pattern and magnitude were more or less similar to those at the surface (Fig 5). At St 1 the north-south component became slightly significant. Also at St 27, tidal current especially northeast-southwest diurnal was more observable than at the surface.

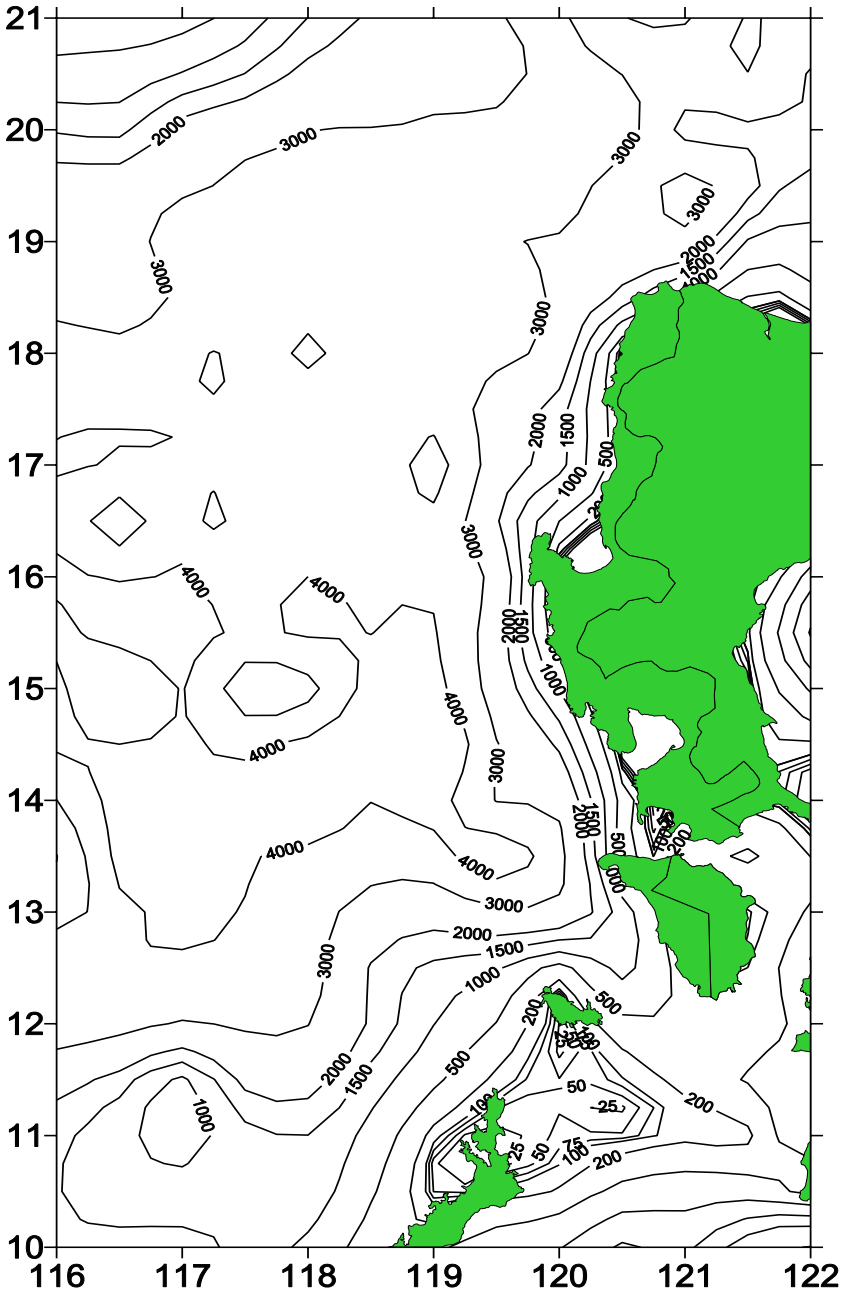

Fig. 1. Bathymetry of the study area.

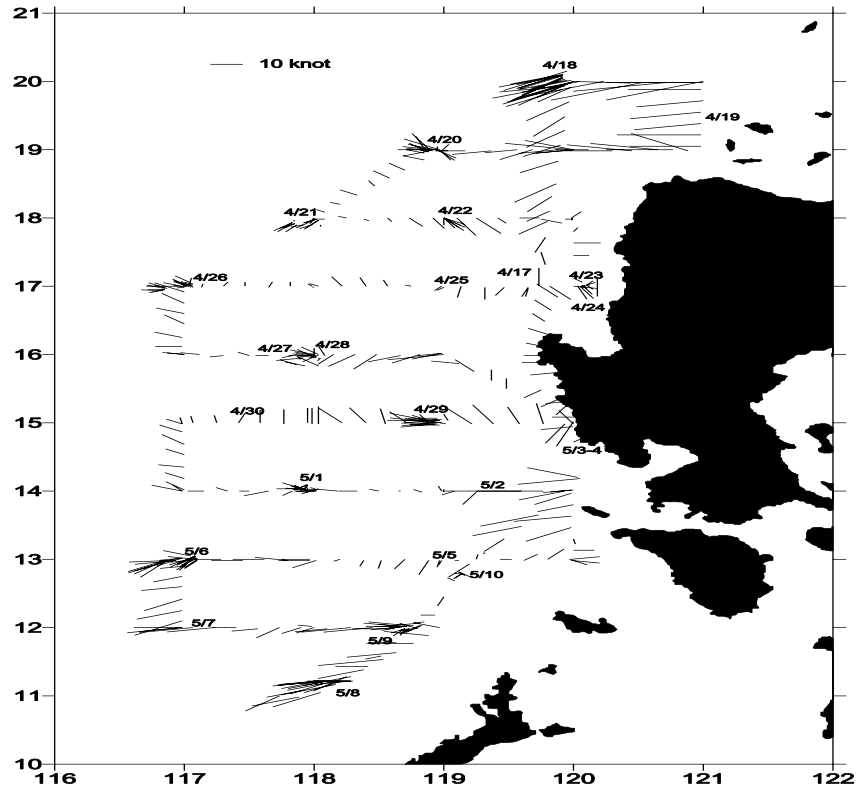

Fig. 2. Hourly wind vector along the cruise track

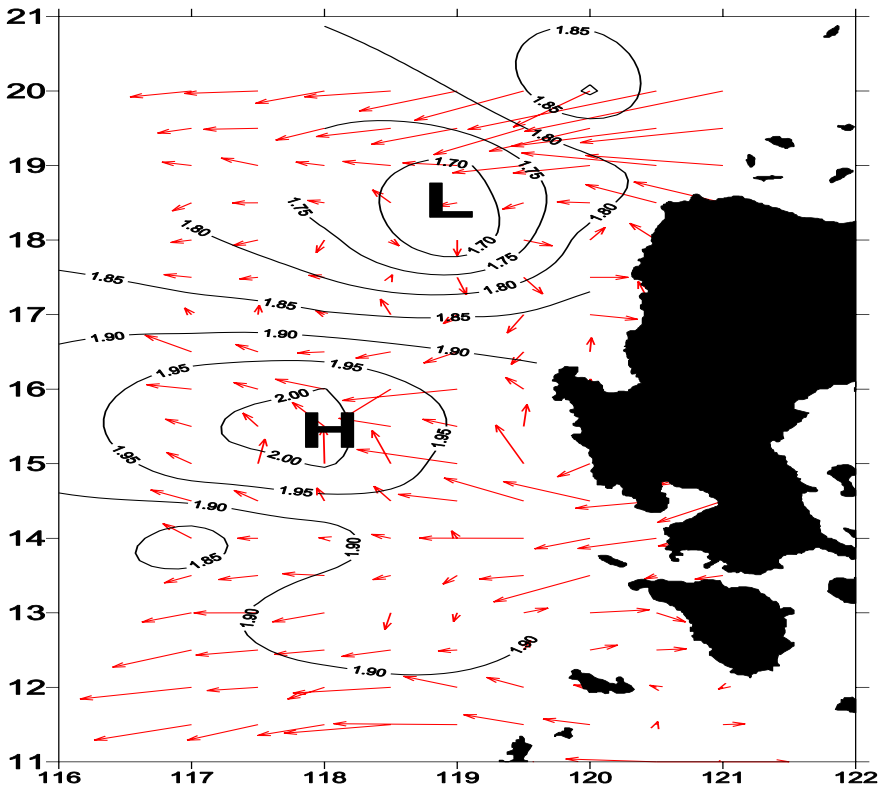

Fig. 3. Dynamic topography (dyn.m) at sea surface relative to 1000 dBar.

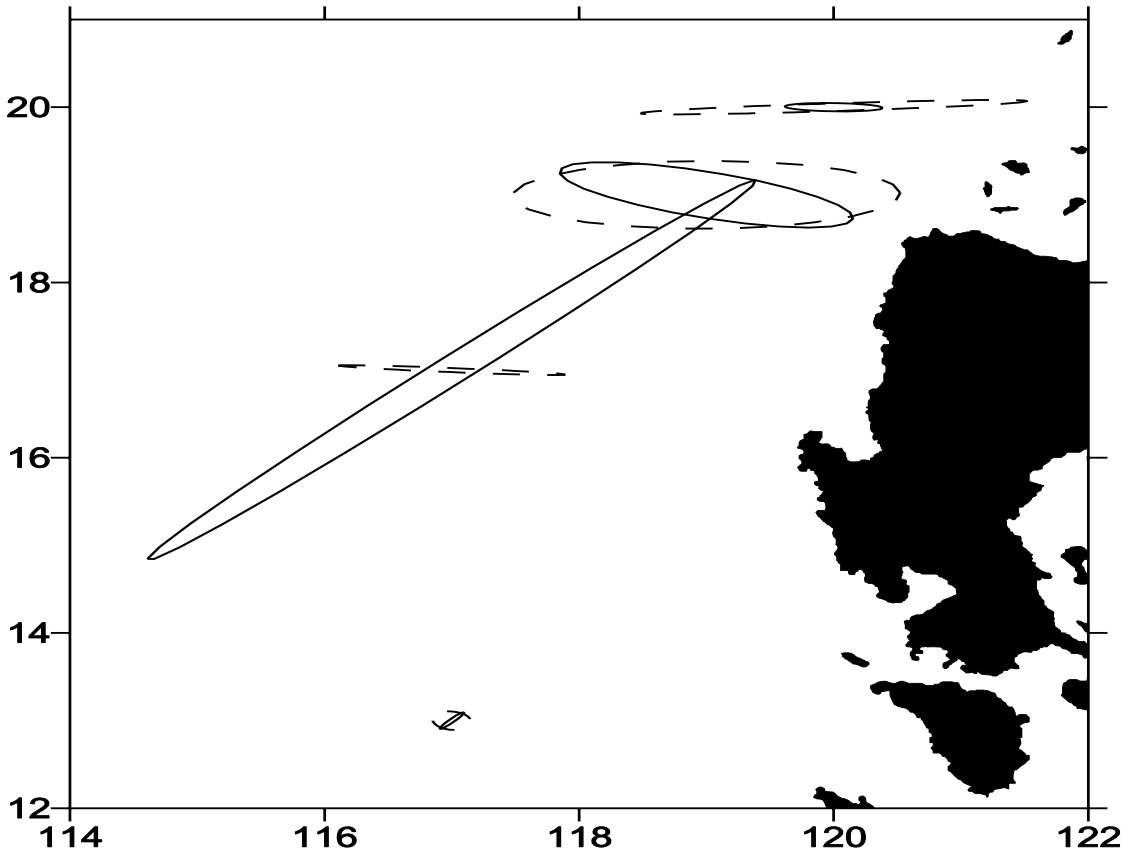

Fig. 4. Diurnal (solid lines) and semidiurnal (dashed lines) components of tidal current at sea surface

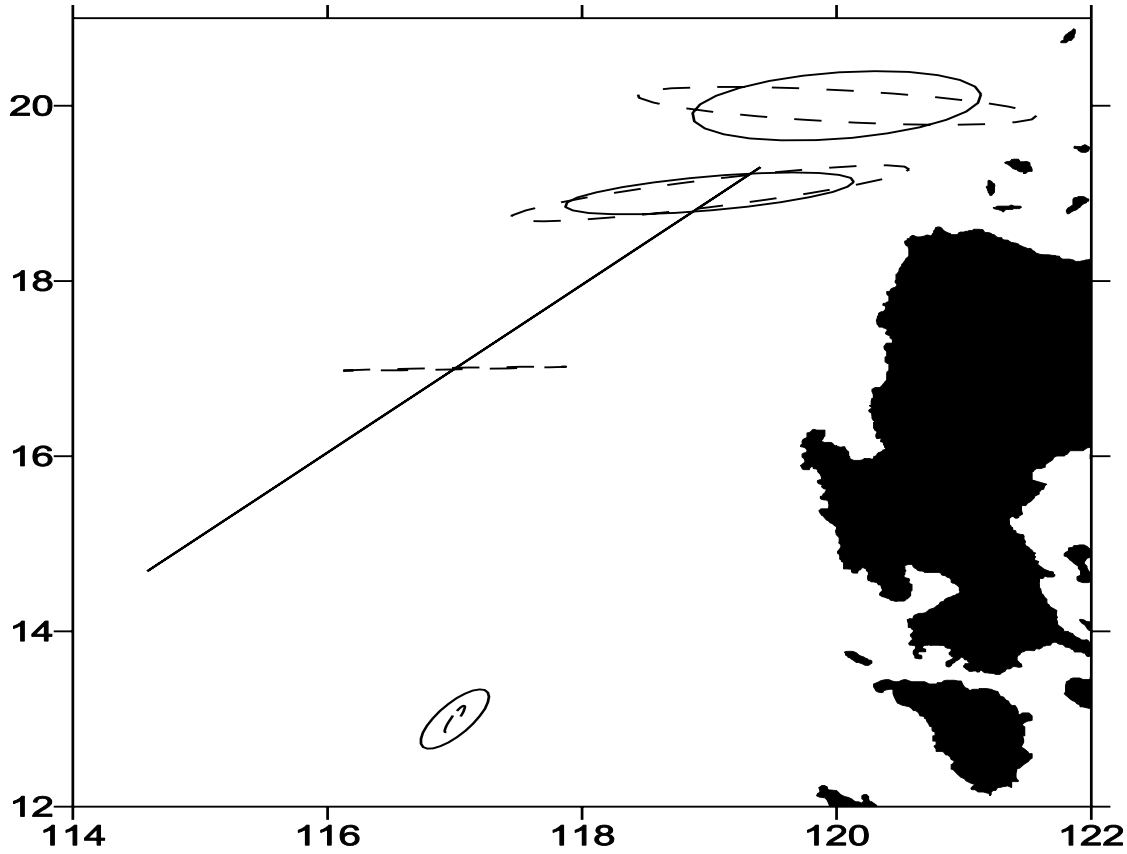

Fig. 5. Diurnal (solid lines) and semidiurnal (dashed lines) components of tidal current at 50m

Discussion

The dynamic high and low in this study area were owed to the relative vertical movement of water. The high area reflected a downward movement or downwelling in which as far as fisheries is concerned, less potential for fisheries. The low dynamic surface due to cyclonic eddy caused by wind turbulence near the head of Luzon Island indicated a potential fishing ground for this season.

Wind-dominated circulation with some orographic effects suggested that potential fishing ground might be located for each season from wind data from coastal as well as ship (GTS) stations. Topex/Poseidon data was attempted in this study, however it was soon found out that the global tidal model used by NASA could not resolve the temporal tidal effect (Fig 6). The lack of reliable tidal data for the area prohibited the usefulness of remote sensing data.

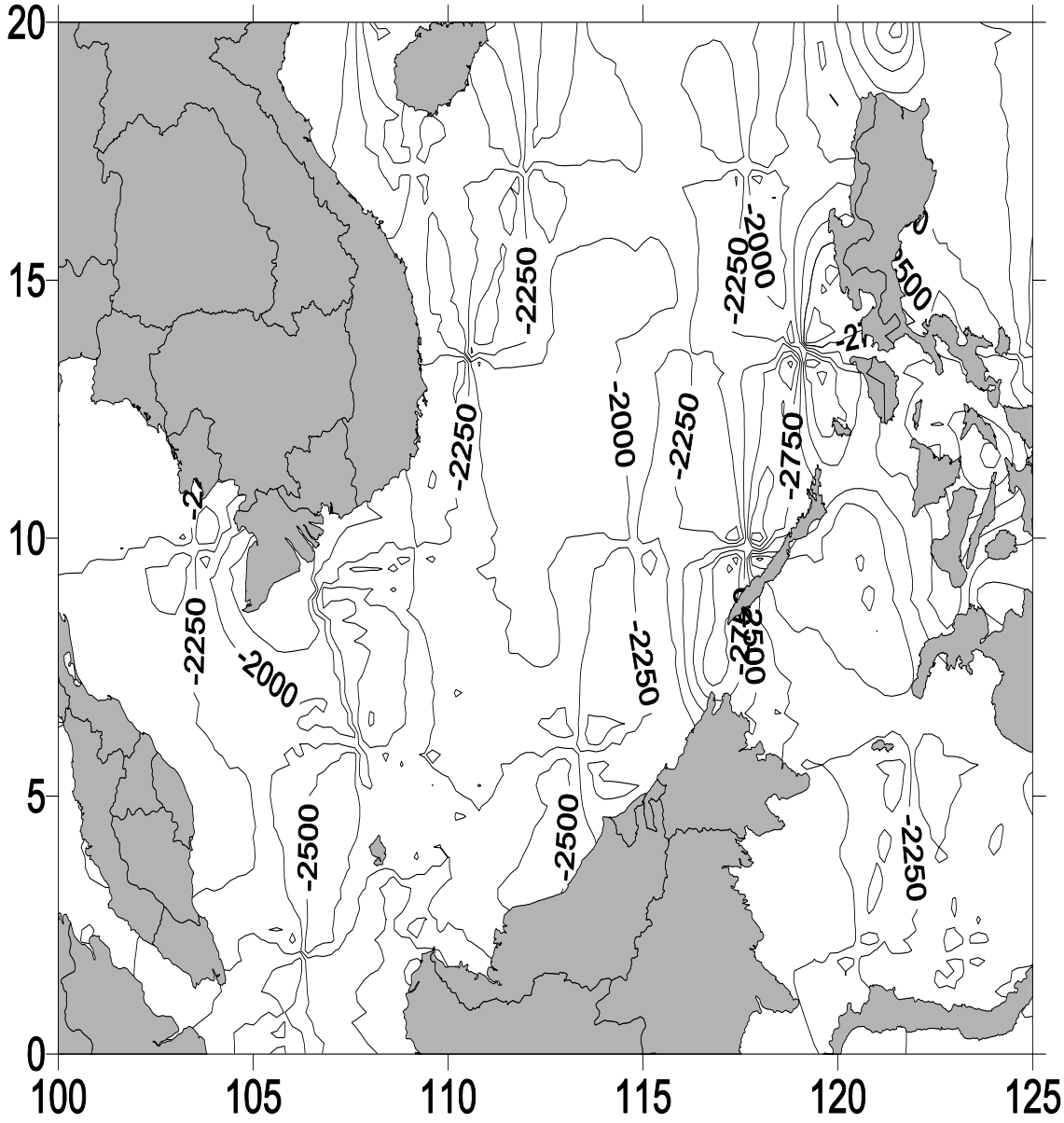

Fig. 6. Sea surface topograhy from Topex/Poseidon. Sea surface was corrected using NASA global tidal model. Yet Troughs ridges were still prominaent